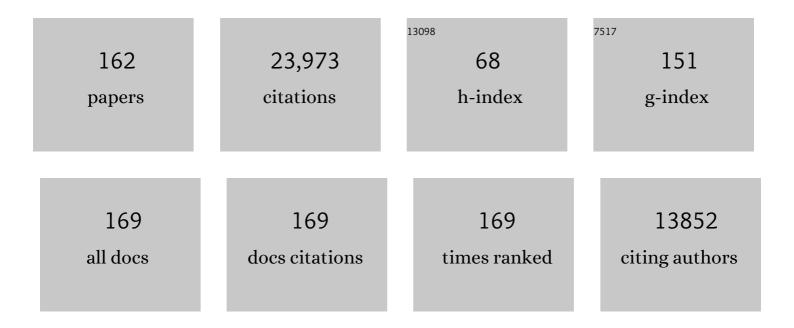
## Robert Tycko

List of Publications by Year in descending order

Source: https://exaly.com/author-pdf/976113/publications.pdf Version: 2024-02-01



#	Article	IF	CITATIONS
1	A structural model for Alzheimer's β-amyloid fibrils based on experimental constraints from solid state NMR. Proceedings of the National Academy of Sciences of the United States of America, 2002, 99, 16742-16747.	7.1	1,757
2	Cell-free Formation of RNA Granules: Low Complexity Sequence Domains Form Dynamic Fibers within Hydrogels. Cell, 2012, 149, 753-767.	28.9	1,725
3	Self-Propagating, Molecular-Level Polymorphism in Alzheimer's ß-Amyloid Fibrils. Science, 2005, 307, 262-265.	12.6	1,587
4	Molecular structural basis for polymorphism in Alzheimer's β-amyloid fibrils. Proceedings of the National Academy of Sciences of the United States of America, 2008, 105, 18349-18354.	7.1	1,046
5	Experimental Constraints on Quaternary Structure in Alzheimer's β-Amyloid Fibrilsâ€. Biochemistry, 2006, 45, 498-512.	2.5	1,019
6	Molecular Structure of β-Amyloid Fibrils in Alzheimer's Disease Brain Tissue. Cell, 2013, 154, 1257-1268.	28.9	986
7	Amyloid Fibril Formation by Aβ16-22, a Seven-Residue Fragment of the Alzheimer's β-Amyloid Peptide, and Structural Characterization by Solid State NMRâ€. Biochemistry, 2000, 39, 13748-13759.	2.5	683
8	Structure of FUS Protein Fibrils and Its Relevance to Self-Assembly and Phase Separation of Low-Complexity Domains. Cell, 2017, 171, 615-627.e16.	28.9	605
9	Peptide Conformation and Supramolecular Organization in Amylin Fibrils:  Constraints from Solid-State NMR. Biochemistry, 2007, 46, 13505-13522.	2.5	542
10	Structural variation in amyloid-β fibrils from Alzheimer's disease clinical subtypes. Nature, 2017, 541, 217-221.	27.8	528
11	Solid-State NMR Studies of Amyloid Fibril Structure. Annual Review of Physical Chemistry, 2011, 62, 279-299.	10.8	493
12	Molecular structure of amyloid fibrils: insights from solid-state NMR. Quarterly Reviews of Biophysics, 2006, 39, 1-55.	5.7	486
13	Progress towards a molecular-level structural understanding of amyloid fibrils. Current Opinion in Structural Biology, 2004, 14, 96-103.	5.7	365
14	Alignment of Biopolymers in Strained Gels:Â A New Way To Create Detectable Dipoleâ^'Dipole Couplings in High-Resolution Biomolecular NMR. Journal of the American Chemical Society, 2000, 122, 9340-9341.	13.7	350
15	Amyloid Polymorphism: Structural Basis and Neurobiological Relevance. Neuron, 2015, 86, 632-645.	8.1	347
16	Antiparallel β-sheet architecture in Iowa-mutant β-amyloid fibrils. Proceedings of the National Academy of Sciences of the United States of America, 2012, 109, 4443-4448.	7.1	316
17	Supramolecular Structure in Full-Length Alzheimer's β-Amyloid Fibrils: Evidence for a Parallel β-Sheet Organization from Solid-State Nuclear Magnetic Resonance. Biophysical Journal, 2002, 83, 1205-1216.	0.5	309
18	Seeded growth of β-amyloid fibrils from Alzheimer's brain-derived fibrils produces a distinct fibril structure. Proceedings of the National Academy of Sciences of the United States of America, 2009, 106, 7443-7448.	7.1	303

#	Article	IF	CITATIONS
19	Measurement of nuclear magnetic dipole—dipole couplings in magic angle spinning NMR. Chemical Physics Letters, 1990, 173, 461-465.	2.6	284
20	Amyloid of the prion domain of Sup35p has an in-register parallel beta-sheet structure. Proceedings of the United States of America, 2006, 103, 19754-19759.	7.1	280
21	Supramolecular Structural Constraints on Alzheimer's β-Amyloid Fibrils from Electron Microscopy and Solid-State Nuclear Magnetic Resonance. Biochemistry, 2002, 41, 15436-15450.	2.5	270
22	Molecular Structures of Amyloid and Prion Fibrils: Consensus versus Controversy. Accounts of Chemical Research, 2013, 46, 1487-1496.	15.6	254
23	Measurement of sample temperatures under magic-angle spinning from the chemical shift and spin-lattice relaxation rate of 79Br in KBr powder. Journal of Magnetic Resonance, 2009, 196, 84-87.	2.1	253
24	Molecular Dynamics Simulations of Alzheimer's β-Amyloid Protofilaments. Journal of Molecular Biology, 2005, 353, 804-821.	4.2	250
25	Sensitivity Enhancement in Solid State 15N NMR by Indirect Detection with High-Speed Magic Angle Spinning. Journal of Magnetic Resonance, 2000, 142, 199-204.	2.1	244
26	Aβ40-Lactam(D23/K28) Models a Conformation Highly Favorable for Nucleation of Amyloid. Biochemistry, 2005, 44, 6003-6014.	2.5	241
27	Adiabatic Rotational Splittings and Berry's Phase in Nuclear Quadrupole Resonance. Physical Review Letters, 1987, 58, 2281-2284.	7.8	228
28	Insights into the Amyloid Folding Problem from Solid-State NMR. Biochemistry, 2003, 42, 3151-3159.	2.5	212
29	Physical and structural basis for polymorphism in amyloid fibrils. Protein Science, 2014, 23, 1528-1539.	7.6	206
30	Theory for cross effect dynamic nuclear polarization under magic-angle spinning in solid state nuclear magnetic resonance: The importance of level crossings. Journal of Chemical Physics, 2012, 137, 084508.	3.0	200
31	Polymorphic Fibril Formation by Residues 10–40 of the Alzheimer's β-Amyloid Peptide. Biophysical Journal, 2006, 90, 4618-4629.	0.5	196
32	Symmetry principles in the design of pulse sequences for structural measurements in magic angle spinning nuclear magnetic resonance. Journal of Chemical Physics, 1993, 98, 932-943.	3.0	183
33	Sensitivity Enhancement in Solid-State13C NMR of Synthetic Polymers and Biopolymers by1H NMR Detection with High-Speed Magic Angle Spinning. Journal of the American Chemical Society, 2001, 123, 2921-2922.	13.7	165
34	Low-temperature dynamic nuclear polarization at 9.4 T with a 30 mW microwave source. Journal of Magnetic Resonance, 2010, 204, 303-313.	2.1	155
35	Characterization of β-Sheet Structure in Ure2p <sub>1</sub> <sub>-</sub> <sub>89</sub> Yeast Prion Fibrils by Solid-State Nuclear Magnetic Resonance. Biochemistry, 2007, 46, 13149-13162.	2.5	154
36	Amyloid of Rnq1p, the basis of the [ <i>PIN</i> <sup>+</sup> ] prion, has a parallel in-register β-sheet structure. Proceedings of the National Academy of Sciences of the United States of America, 2008, 105, 2403-2408.	7.1	141

#	Article	IF	CITATIONS
37	Polymorph-Specific Kinetics and Thermodynamics of β-Amyloid Fibril Growth. Journal of the American Chemical Society, 2013, 135, 6860-6871.	13.7	141
38	Recoupling of chemical shift anisotropies in solid-state NMR under high-speed magic-angle spinning and in uniformly 13C-labeled systems. Journal of Chemical Physics, 2003, 118, 8378-8389.	3.0	139
39	The α-Helical C-Terminal Domain of Full-Length Recombinant PrP Converts to an In-Register Parallel β-Sheet Structure in PrP Fibrils: Evidence from Solid State Nuclear Magnetic Resonance. Biochemistry, 2010, 49, 9488-9497.	2.5	135
40	Parallel β-Sheets and Polar Zippers in Amyloid Fibrils Formed by Residues 10â^'39 of the Yeast Prion Protein Ure2p. Biochemistry, 2005, 44, 10669-10680.	2.5	134
41	Perturbation of nuclear spin polarizations in solid state NMR of nitroxide-doped samples by magic-angle spinning without microwaves. Journal of Chemical Physics, 2014, 140, 184201.	3.0	133
42	Evidence for Novel β-Sheet Structures in Iowa Mutant β-Amyloid Fibrils. Biochemistry, 2009, 48, 6072-6084.	2.5	132
43	Measurement of amyloid fibril mass-per-length by tilted-beam transmission electron microscopy. Proceedings of the National Academy of Sciences of the United States of America, 2009, 106, 14339-14344.	7.1	122
44	Double-quantum filtering in magic-angle-spinning NMR spectroscopy: an approach to spectral simplification and molecular structure determination. Journal of the American Chemical Society, 1991, 113, 9444-9448.	13.7	121
45	Determination of Peptide Conformations by Two-Dimensional Magic Angle Spinning NMR Exchange Spectroscopy with Rotor Synchronization. Journal of the American Chemical Society, 1996, 118, 8487-8488.	13.7	121
46	Increasing the Amphiphilicity of an Amyloidogenic Peptide Changes the β-Sheet Structure in the Fibrils from Antiparallel to Parallel. Biophysical Journal, 2004, 86, 428-434.	0.5	119
47	The Functional Curli Amyloid Is Not Based on In-register Parallel β-Sheet Structure. Journal of Biological Chemistry, 2009, 284, 25065-25076.	3.4	119
48	Symmetry-based constant-time homonuclear dipolar recoupling in solid state NMR. Journal of Chemical Physics, 2007, 126, 064506.	3.0	117
49	Molecular structure of monomorphic peptide fibrils within a kinetically trapped hydrogel network. Proceedings of the National Academy of Sciences of the United States of America, 2015, 112, 9816-9821.	7.1	117
50	BIOMOLECULAR SOLID STATE NMR: Advances in Structural Methodology and Applications to Peptide and Protein Fibrils. Annual Review of Physical Chemistry, 2001, 52, 575-606.	10.8	115
51	Constraints on Supramolecular Structure in Amyloid Fibrils from Two-Dimensional Solid-State NMR Spectroscopy with Uniform Isotopic Labeling. Journal of the American Chemical Society, 2003, 125, 6606-6607.	13.7	111
52	Molecular structure of a prevalent amyloid-β fibril polymorph from Alzheimer's disease brain tissue. Proceedings of the National Academy of Sciences of the United States of America, 2021, 118, .	7.1	108
53	Molecular, Local, and Network-Level Basis for the Enhanced Stiffness of Hydrogel Networks Formed from Coassembled Racemic Peptides: Predictions from Pauling and Corey. ACS Central Science, 2017, 3, 586-597.	11.3	107
54	Successive Stages of Amyloid-β Self-Assembly Characterized by Solid-State Nuclear Magnetic Resonance with Dynamic Nuclear Polarization. Journal of the American Chemical Society, 2015, 137, 8294-8307.	13.7	103

#	Article	IF	CITATIONS
55	Investigation of molecular structure in solids by twoâ€dimensional NMR exchange spectroscopy with magic angle spinning. Journal of Chemical Physics, 1996, 105, 7915-7930.	3.0	97
56	Biomolecular solid state NMR with magic-angle spinning at 25K. Journal of Magnetic Resonance, 2008, 195, 179-186.	2.1	97
57	Biopolymer Conformational Distributions from Solid-State NMR: α-Helix and 310-Helix Contents of a Helical Peptide. Journal of the American Chemical Society, 1998, 120, 7039-7048.	13.7	94
58	Controlling residual dipolar couplings in high-resolution NMR of proteins by strain induced alignment in a gel. Journal of Biomolecular NMR, 2001, 21, 141-151.	2.8	94
59	Structural Evolution of Iowa Mutant β-Amyloid Fibrils from Polymorphic to Homogeneous States under Repeated Seeded Growth. Journal of the American Chemical Society, 2011, 133, 4018-4029.	13.7	92
60	Probing site-specific conformational distributions in protein folding with solid-state NMR. Proceedings of the National Academy of Sciences of the United States of America, 2005, 102, 3284-3289.	7.1	91
61	Two Prion Variants of Sup35p Have In-Register Parallel β-Sheet Structures, Independent of Hydration. Biochemistry, 2009, 48, 5074-5082.	2.5	89
62	The Japanese Mutant Aβ (ΔE22-Aβ <sub>1â~'39</sub> ) Forms Fibrils Instantaneously, with Low-Thioflavin T Fluorescence: Seeding of Wild-Type Aβ <sub>1â~'40</sub> into Atypical Fibrils by ΔE22-Aβ <sub>1â~'39</sub> . Biochemistry, 2011, 50, 2026-2039.	2.5	88
63	Solid-state NMR in biological and materials physics. Physics Today, 2009, 62, 44-49.	0.3	84
64	Detection of a Transient Intermediate in a Rapid Protein Folding Process by Solid-State Nuclear Magnetic Resonance. Journal of the American Chemical Society, 2010, 132, 24-25.	13.7	83
65	Optical Pumping in Solid State Nuclear Magnetic Resonance. The Journal of Physical Chemistry, 1996, 100, 13240-13250.	2.9	79
66	Solid-state NMR evidence for an antibody-dependent conformation of the V3 loop of HIV-1 gp120. Nature Structural Biology, 1999, 6, 141-145.	9.7	78
67	Site-Specific Identification of Non-β-Strand Conformations in Alzheimer's β-Amyloid Fibrils by Solid-State NMR. Biophysical Journal, 2003, 84, 3326-3335.	0.5	78
68	Molecular structure and interactions within amyloid-like fibrils formed by a low-complexity protein sequence from FUS. Nature Communications, 2020, 11, 5735.	12.8	76
69	Quantitative Conformational Measurements in Solid State NMR by Constant-Time Homonuclear Dipolar Recoupling. Journal of the American Chemical Society, 1998, 120, 4897-4898.	13.7	72
70	Molecular Structure of Aggregated Amyloid-β: Insights from Solid-State Nuclear Magnetic Resonance. Cold Spring Harbor Perspectives in Medicine, 2016, 6, a024083.	6.2	71
71	NMR Studies of Chloroquineâ^'Ferriprotoporphyrin IX Complex. Journal of Physical Chemistry A, 2003, 107, 5821-5825.	2.5	69
72	Optical pumping in indium phosphide: 31P NMR measurements and potential for signal enhancement in biological solid state NMR. Solid State Nuclear Magnetic Resonance, 1998, 11, 1-9.	2.3	67

#	Article	IF	CITATIONS
73	Locating folds of the in-register parallel β-sheet of the Sup35p prion domain infectious amyloid. Proceedings of the National Academy of Sciences of the United States of America, 2014, 111, E4615-22.	7.1	67
74	Measurement of dipole-coupled lineshapes in a many-spin system by constant-time two-dimensional solid state NMR with high-speed magic-angle spinning. Chemical Physics, 2001, 266, 231-236.	1.9	66
75	Solid state nuclear magnetic resonance with magic-angle spinning and dynamic nuclear polarization below 25K. Journal of Magnetic Resonance, 2013, 226, 100-106.	2.1	66
76	Structure and Dynamics of the HIV-1 Vpu Transmembrane Domain Revealed by Solid-State NMR with Magic-Angle Spinningâ€. Biochemistry, 2006, 45, 918-933.	2.5	65
77	NMR at Low and Ultralow Temperatures. Accounts of Chemical Research, 2013, 46, 1923-1932.	15.6	64
78	Amyloids of Shuffled Prion Domains That Form Prions Have a Parallel In-Register β-Sheet Structureâ€. Biochemistry, 2008, 47, 4000-4007.	2.5	63
79	Low-temperature dynamic nuclear polarization with helium-cooled samples and nitrogen-driven magic-angle spinning. Journal of Magnetic Resonance, 2016, 264, 99-106.	2.1	63
80	High-order multiple quantum excitation in 13C nuclear magnetic resonance spectroscopy of organic solids. Journal of Chemical Physics, 1999, 110, 2749-2752.	3.0	62
81	Determination of Polypeptide Backbone Dihedral Angles in Solid State NMR by Double Quantum 13C Chemical Shift Anisotropy Measurements. Journal of Magnetic Resonance, 2001, 149, 131-138.	2.1	62
82	Oligomerization state and supramolecular structure of the HIVâ€1 Vpu protein transmembrane segment in phospholipid bilayers. Protein Science, 2010, 19, 1877-1896.	7.6	60
83	Segmental Polymorphism in a Functional Amyloid. Biophysical Journal, 2011, 101, 2242-2250.	0.5	59
84	Frequency-selective homonuclear dipolar recoupling in solid state NMR. Journal of Chemical Physics, 2006, 124, 194303.	3.0	58
85	Sensitivity Enhancement in Structural Measurements by Solid State NMR through Pulsed Spin Locking. Journal of Magnetic Resonance, 2002, 155, 293-299.	2.1	57
86	The Core of Ure2p Prion Fibrils Is Formed by the N-Terminal Segment in a Parallel Cross-Î <sup>2</sup> Structure: Evidence from Solid-State NMR. Journal of Molecular Biology, 2011, 409, 263-277.	4.2	56
87	Molecular Alignment within β-Sheets in Aβ14-23 Fibrils: Solid-State NMR Experiments and Theoretical Predictions. Biophysical Journal, 2007, 92, 594-602.	0.5	51
88	Simulated Self-Assembly of the HIV-1 Capsid: Protein Shape and Native Contacts Are Sufficient for Two-Dimensional Lattice Formation. Biophysical Journal, 2011, 100, 3035-3044.	0.5	51
89	Zero field nuclear magnetic resonance in high field. Journal of Chemical Physics, 1990, 92, 5776-5793.	3.0	50
90	Prospects for resonance assignments in multidimensional solid-state NMR spectra of uniformly labeled proteins. Journal of Biomolecular NMR, 1996, 8, 239-251.	2.8	50

#	Article	IF	CITATIONS
91	Solid-State NMR Spectroscopy Method for Determination of the Backbone Torsion Angle Ï^ in Peptides with Isolated Uniformly Labeled Residues. Journal of the American Chemical Society, 2003, 125, 11828-11829.	13.7	50
92	Structural characterization of the D290V mutation site in hnRNPA2 low-complexity–domain polymers. Proceedings of the National Academy of Sciences of the United States of America, 2018, 115, E9782-E9791.	7.1	50
93	Stray-field NMR imaging and wavelength dependence of optically pumped nuclear spin polarization in InP. Physical Review B, 1999, 60, 8672-8679.	3.2	49
94	Solid-State NMR Yields Structural Constraints on the V3 Loop from HIV-1 Gp120 Bound to the 447-52D Antibody Fv Fragment. Journal of the American Chemical Society, 2004, 126, 4979-4990.	13.7	49
95	Structural and dynamical characterization of tubular HIVâ€1 capsid protein assemblies by solid state nuclear magnetic resonance and electron microscopy. Protein Science, 2010, 19, 716-730.	7.6	49
96	An Achilles' Heel in an Amyloidogenic Protein and Its Repair. Journal of Biological Chemistry, 2010, 285, 10806-10821.	3.4	49
97	Site-Specific Structural Variations Accompanying Tubular Assembly of the HIV-1 Capsid Protein. Journal of Molecular Biology, 2014, 426, 1109-1127.	4.2	49
98	Nuclear magnetic resonance crystallography: molecular orientational ordering in three forms of solid methanol. Journal of the American Chemical Society, 1991, 113, 3592-3593.	13.7	48
99	A Monte Carlo/simulated annealing algorithm for sequential resonance assignment in solid state NMR of uniformly labeled proteins with magic-angle spinning. Journal of Magnetic Resonance, 2010, 205, 304-314.	2.1	48
100	Solid-state NMR data support a helix-loop-helix structural model for the N-terminal half of HIV-1 rev in fibrillar form. Journal of Molecular Biology, 2001, 313, 845-859.	4.2	47
101	Expression and purification of a recombinant peptide from the Alzheimer's β-amyloid protein for solid-state NMR. Protein Expression and Purification, 2005, 42, 200-210.	1.3	46
102	Repeat Domains of Melanosome Matrix Protein Pmel17 Orthologs Form Amyloid Fibrils at the Acidic Melanosomal pH. Journal of Biological Chemistry, 2011, 286, 8385-8393.	3.4	45
103	A general Monte Carlo/simulated annealing algorithm for resonance assignment in NMR of uniformly labeled biopolymers. Journal of Biomolecular NMR, 2011, 50, 267-276.	2.8	42
104	Application of millisecond time-resolved solid state NMR to the kinetics and mechanism of melittin self-assembly. Proceedings of the National Academy of Sciences of the United States of America, 2019, 116, 16717-16722.	7.1	42
105	Characterization of Amyloid Structures at the Molecular Level by Solid State Nuclear Magnetic Resonance Spectroscopy. Methods in Enzymology, 2006, 413, 103-122.	1.0	41
106	Quantitative Determination of Site-Specific Conformational Distributions in an Unfolded Protein by Solid-State Nuclear Magnetic Resonance. Journal of Molecular Biology, 2009, 392, 1055-1073.	4.2	41
107	Structure of aggregates revealed. Nature, 2016, 537, 492-493.	27.8	38
108	Synthesis and evaluation of nitroxide-based oligoradicals for low-temperature dynamic nuclear polarization in solid state NMR. Journal of Magnetic Resonance, 2014, 244, 98-106.	2.1	36

#	Article	IF	CITATIONS
109	Solid-State NMR as a Probe of Amyloid Structure. Protein and Peptide Letters, 2006, 13, 229-234.	0.9	35
110	Evidence from Solid-State NMR for Nonhelical Conformations in the Transmembrane Domain of the Amyloid Precursor Protein. Biophysical Journal, 2011, 100, 711-719.	0.5	35
111	Helical Conformation in the CA-SP1 Junction of the Immature HIV-1 Lattice Determined from Solid-State NMR of Virus-like Particles. Journal of the American Chemical Society, 2016, 138, 12029-12032.	13.7	35
112	Multidimensional Heteronuclear Correlation Spectroscopy of a Uniformly15N- and13C-Labeled Peptide Crystal:Â Toward Spectral Resolution, Assignment, and Structure Determination of Oriented Molecules in Solid-State NMR. Journal of the American Chemical Society, 2000, 122, 1443-1455.	13.7	34
113	Fiber Diffraction Data Indicate a Hollow Core for the Alzheimer's AÎ <sup>2</sup> 3-Fold Symmetric Fibril. Journal of Molecular Biology, 2012, 423, 454-461.	4.2	34
114	Stochastic Dipolar Recoupling in Nuclear Magnetic Resonance of Solids. Physical Review Letters, 2007, 99, 187601.	7.8	32
115	Dynamic nuclear polarization-enhanced 1H–13C double resonance NMR in static samples below 20 K. Journal of Magnetic Resonance, 2012, 221, 32-40.	2.1	32
116	Transiently structured head domains control intermediate filament assembly. Proceedings of the National Academy of Sciences of the United States of America, 2021, 118, .	7.1	32
117	Segmental isotopic labeling of HIV-1 capsid protein assemblies for solid state NMR. Journal of Biomolecular NMR, 2018, 70, 103-114.	2.8	31
118	Side Chain Hydrogen-Bonding Interactions within Amyloid-like Fibrils Formed by the Low-Complexity Domain of FUS: Evidence from Solid State Nuclear Magnetic Resonance Spectroscopy. Biochemistry, 2020, 59, 364-378.	2.5	31
119	Zero-Field Nuclear Magnetic Resonance in High Field: The Untruncation of Dipole-Dipole Couplings by Coherent Averaging. Physical Review Letters, 1988, 60, 2734-2737.	7.8	29
120	Experimentally Derived Structural Constraints for Amyloid Fibrils of Wild-Type Transthyretin. Biophysical Journal, 2011, 101, 2485-2492.	0.5	29
121	On Mechanisms of Dynamic Nuclear Polarization in Solids. Israel Journal of Chemistry, 2014, 54, 39-46.	2.3	28
122	Time-resolved DEER EPR and solid-state NMR afford kinetic and structural elucidation of substrate binding to Ca <sup>2+</sup> -ligated calmodulin. Proceedings of the National Academy of Sciences of the United States of America, 2022, 119, .	7.1	28
123	Absolute Structural Constraints on Amyloid Fibrils from Solid-State NMR Spectroscopy of Partially Oriented Samples. Journal of the American Chemical Society, 2004, 126, 4478-4479.	13.7	27
124	What can solid state NMR contribute to our understanding of protein folding?. Biophysical Chemistry, 2010, 151, 10-21.	2.8	27
125	Probing hydrogen bonds in the antibody-bound HIV-1 gp120 V3 loop by solid state NMR REDOR measurements. Journal of Biomolecular NMR, 2000, 16, 313-327.	2.8	26
126	Zero-quantum frequency-selective recoupling of homonuclear dipole-dipole interactions in solid state nuclear magnetic resonance. Journal of Chemical Physics, 2009, 131, 045101.	3.0	26

#	Article	IF	CITATIONS
127	Coexisting order and disorder within a common 40-residue amyloid-Î <sup>2</sup> fibril structure in Alzheimer's disease brain tissue. Chemical Communications, 2018, 54, 5070-5073.	4.1	26
128	Prospects for sub-micron solid state nuclear magnetic resonance imaging with low-temperature dynamic nuclear polarization. Physical Chemistry Chemical Physics, 2010, 12, 5779.	2.8	25
129	Restraints on backbone conformations in solid state NMR studies of uniformly labeled proteins from quantitative amide 15N–15N and carbonyl 13C–13C dipolar recoupling data. Journal of Magnetic Resonance, 2012, 218, 115-127.	2.1	23
130	Dynamic nuclear polarization-enhanced 13C NMR spectroscopy of static biological solids. Journal of Magnetic Resonance, 2013, 231, 5-14.	2.1	23
131	Structural differences in amyloid-β fibrils from brains of nondemented elderly individuals and Alzheimer's disease patients. Proceedings of the National Academy of Sciences of the United States of America, 2021, 118, .	7.1	23
132	Theory of Stochastic Dipolar Recoupling in Solid-State Nuclear Magnetic Resonanceâ€. Journal of Physical Chemistry B, 2008, 112, 6114-6121.	2.6	22
133	Millisecond Time-Resolved Solid-State NMR Reveals a Two-Stage Molecular Mechanism for Formation of Complexes between Calmodulin and a Target Peptide from Myosin Light Chain Kinase. Journal of the American Chemical Society, 2020, 142, 21220-21232.	13.7	22
134	Dual Processing of Two-Dimensional Exchange Data in Magic Angle Spinning NMR of Solids. Journal of Magnetic Resonance, 1999, 141, 141-147.	2.1	20
135	Micron-scale magnetic resonance imaging of both liquids and solids. Journal of Magnetic Resonance, 2015, 260, 1-9.	2.1	20
136	Structure of the Dimerization Interface in the Mature HIV-1 Capsid Protein Lattice from Solid State NMR of Tubular Assemblies. Journal of the American Chemical Society, 2016, 138, 8538-8546.	13.7	20
137	Effects of an HIV-1 maturation inhibitor on the structure and dynamics of CA-SP1 junction helices in virus-like particles. Proceedings of the National Academy of Sciences of the United States of America, 2020, 117, 10286-10293.	7.1	19
138	Sensitivity Enhancement in Two-Dimensional Solid-State NMR Spectroscopy by Transverse Mixing. ChemPhysChem, 2004, 5, 863-868.	2.1	18
139	Rotational resonance in uniformly 13C-labeled solids: effects on high-resolution magic-angle spinning NMR spectra and applications in structural studies of biomolecular systems. Journal of Magnetic Resonance, 2004, 168, 137-146.	2.1	18
140	Broadband rotational resonance in solid state NMR spectroscopy. Journal of Chemical Physics, 2004, 120, 8349-8352.	3.0	17
141	Constraints on the Structure of Fibrils Formed by a Racemic Mixture of Amyloid-Î <sup>2</sup> Peptides from Solid-State NMR, Electron Microscopy, and Theory. Journal of the American Chemical Society, 2021, 143, 13299-13313.	13.7	17
142	Major Variations in HIV-1 Capsid Assembly Morphologies Involve Minor Variations in Molecular Structures of Structurally Ordered Protein Segments. Journal of Biological Chemistry, 2016, 291, 13098-13112.	3.4	15
143	Optical pumping of dipolar order in a coupled nuclear spin system. Molecular Physics, 1998, 95, 1169-1176.	1.7	14
144	Low-temperature magnetic resonance imaging with 2.8†μm isotropic resolution. Journal of Magnetic Resonance, 2018, 287, 47-55.	2.1	14

#	Article	IF	CITATIONS
145	Introduction to Special Topic: New Developments in Magnetic Resonance. Journal of Chemical Physics, 2008, 128, 052101.	3.0	13
146	Succinyl-DOTOPA: An effective triradical dopant for low-temperature dynamic nuclear polarization with high solubility in aqueous solvent mixtures at neutral pH. Journal of Magnetic Resonance, 2020, 311, 106672.	2.1	11
147	Preparation of Amyloid Fibrils Seeded from Brain and Meninges. Methods in Molecular Biology, 2016, 1345, 299-312.	0.9	11
148	On the problem of resonance assignments in solid state NMR of uniformly 15N,13C-labeled proteins. Journal of Magnetic Resonance, 2015, 253, 166-172.	2.1	10
149	Optimization of band-selective homonuclear dipolar recoupling in solid-state NMR by a numerical phase search. Journal of Chemical Physics, 2019, 150, 154201.	3.0	10
150	Zero-quantum stochastic dipolar recoupling in solid state nuclear magnetic resonance. Journal of Chemical Physics, 2012, 137, 104201.	3.0	7
151	Remote sensing of sample temperatures in nuclear magnetic resonance using photoluminescence of semiconductor quantum dots. Journal of Magnetic Resonance, 2014, 244, 64-67.	2.1	7
152	Temperature-Dependent Nuclear Spin Relaxation Due to Paramagnetic Dopants Below 30 K: Relevance to DNP-Enhanced Magnetic Resonance Imaging. Journal of Physical Chemistry B, 2018, 122, 11731-11742.	2.6	7
153	Depletion of amyloidâ€Î² peptides from solution by sequestration within fibrilâ€seeded hydrogels. Protein Science, 2018, 27, 1218-1230.	7.6	6
154	Enhanced spatial resolution in magnetic resonance imaging by dynamic nuclear polarization at 5 K. Proceedings of the National Academy of Sciences of the United States of America, 2022, 119, .	7.1	6
155	Millisecond Time-Resolved Solid-State NMR Initiated by Rapid Inverse Temperature Jumps. Journal of the American Chemical Society, 2022, 144, 9920-9925.	13.7	6
156	Indirect detection in solid state NMR: An illustrious history and a bright future. Journal of Magnetic Resonance, 2018, 288, 122-123.	2.1	5
157	Slice selection in low-temperature, DNP-enhanced magnetic resonance imaging by Lee-Goldburg spin-locking and phase modulation. Journal of Magnetic Resonance, 2020, 313, 106715.	2.1	5
158	Automated picking of amyloid fibrils from cryo-EM images for helical reconstruction with RELION. Journal of Structural Biology, 2021, 213, 107736.	2.8	5
159	Optical pumping of dipolar order in a coupled nuclear spin system. Molecular Physics, 1998, 95, 1169-1176.	1.7	5
160	Conformational constraints in solid-state NMR of uniformly labeled polypeptides from double single-quantum-filtered rotational echo double resonance. Magnetic Resonance in Chemistry, 2007, 45, S101-S106.	1.9	4
161	β-Amyloid Fibril Structures, In Vitro and In Vivo. Research and Perspectives in Alzheimer's Disease, 2013, , 19-31.	0.1	1
162	Molecular structure of amyloid and prion fibrils. FASEB Journal, 2009, 23, 423.3.	0.5	0